Journal of Experimental Nanoscience
Publication details, including instructions for authors and subscription information:
http://www.informaworld.com/smpp/title~content=t716100757

In vivo biodistribution and toxicity depends on nanomaterial composition, size, surface functionalisation and route of exposure

S. Harper[ab]; C. Usenko[c]; J. E. Hutchison[bd]; B. L. S. Maddux[b]; R. L. Tanguay[ab]
[a] Department of Environmental and Molecular Toxicology, Oregon State University, Corvallis, OR, USA [b] ONAMI Safer Nanomaterials and Nanomanufacturing Initiative, Corvallis, OR, USA [c] Department of Biology, Baylor University, Waco, TX, USA [d] Department of Chemistry, University of Oregon, Eugene, USA

To cite this Article Harper, S. , Usenko, C. , Hutchison, J. E. , Maddux, B. L. S. and Tanguay, R. L.(2008) '*In vivo* biodistribution and toxicity depends on nanomaterial composition, size, surface functionalisation and route of exposure', Journal of Experimental Nanoscience, 3: 3, 195 — 206
To link to this Article: DOI: 10.1080/17458080802378953
URL: http://dx.doi.org/10.1080/17458080802378953

Journal of Experimental Nanoscience
Vol. 3, No. 3, September 2008, 195–206

Taylor & Francis
Taylor & Francis Group

In vivo biodistribution and toxicity depends on nanomaterial composition, size, surface functionalisation and route of exposure

S. Harper[ab]*, C. Usenko[c], J.E. Hutchison[bd], B.L.S. Maddux[b] and R.L. Tanguay[ab]

[a]*Department of Environmental and Molecular Toxicology, Oregon State University, Corvallis, OR, USA;* [b]*ONAMI Safer Nanomaterials and Nanomanufacturing Initiative, University of Oregon, Corvallis, OR, USA;* [c]*Department of Biology, Baylor University, Waco, TX, USA;* [d]*Department of Chemistry, University of Oregon, Eugene, USA*

(*Received 10 April 2008; final version received 18 July 2008*)

Anticipated growth of the nanotechnology industry has motivated the development of rapid, relevant and efficient testing strategies to evaluate the biological activity and toxic potential of the growing number of novel nanoparticles. Since nanoparticles may interact with biological systems in unforeseen ways, it is important that evaluation of nanomaterial–biological interactions cover a broad range of cell types, tissues, organs and systems. Here, we use the embryonic zebrafish as a dynamic whole animal (*in vivo*) assay to investigate the importance of chemical composition, size, surface functionalisation and route of exposure on nanomaterial–biological interactions and delineate nanomaterials that are biologically active from those that are not. Information gained using model systems, such as the embryonic zebrafish, can be used to direct the rational development of safer, less hazardous nanoparticles. Our results demonstrate the utility of this model as an effective and accurate tool to assess the biological activity and toxic potential of nanomaterials in a short period of time with minimal cost.

Keywords: nanotoxicology; carbon fullerene; metal oxide; fluorescent nanomaterials; gold nanoparticles

1. Proactive nanotechnology design

Exploitation of enabling nanotechnologies will provide unprecedented advances in virtually every aspect of science and engineering. The hallmark of nanotechnology is our new-found ability to manipulate matter at the atomic level which allows us to precisely control the physical and chemical properties of nanomaterials. Thus, it should be feasible to minimise deleterious biological impact once the physicochemical properties that dictate adverse biological interactions are identified. Engineers and scientists must work together to provide this critical information to industry so that they can proactively design nanomaterials with enhanced performance and minimal hazard.

*Corresponding author. Email: harpers@science.oregonstate.edu

ISSN 1745–8080 print/ISSN 1745–8099 online

DOI: 10.1080/17458080802378953
http://www.informaworld.com

2. Model system for testing nanomaterial–biological interactions

Various biological models have been employed for toxicological evaluations. Like many models, much of the anatomy and physiology of fish is highly homologous to humans [1]. Zebrafish have been successfully used as an *in vivo* model organism for predictive toxicology and are now proving invaluable for the pharmaceutical and biotechnology industries for evaluating integrated system effects [2–4]. A remarkable similarity in cellular structure, signalling processes, anatomy and physiology exists among zebrafish and other high-order vertebrates [5]. Zebrafish also possess all of the classical sense modalities, including vision, olfaction, taste, touch, balance and hearing; and their sensory pathways share an overall homology with humans [1,6].

2.1. *Inherent advantages of zebrafish*

Numerous features of zebrafish biology (e.g. small size, rapid embryonic development, short life cycle) make this model system logistically attractive to rapidly evaluate nanoparticle–biological interactions [6]. Females produce hundreds of eggs weekly, so large sample sizes are easily achieved for statistically powerful dose-response studies [7]. This abundant supply of embryos also makes it possible to simultaneously assess the toxicity of a large number of nanomaterials in a short period of time. Zebrafish embryos develop externally and are optically transparent so it is possible to resolve individual cells *in vivo* across a broad range of developmental stages or throughout the duration of an experimental exposure using simple microscopic techniques. Resolution of specific cell populations can be increased by the use of transgenic zebrafish models that express fluorescent carbon fullerene reporter genes in cell types of interest [8]. Finally, assay volumes using the zebrafish model are small; thus, only limited amounts of nanoparticles/nanomaterials are needed to evaluate biological responses.

2.2. *Testing for nanomaterial toxicity during embryonic life stage*

We investigate whole animal biological responses (i.e. organismal uptake, systemic distribution and toxicological effects) by detailing the effects of nanoparticle exposure on embryonic zebrafish. Our experimental design tests for nanomaterial toxicity during early vertebrate development for two important reasons. First, fundamental processes of development are highly conserved across species [9–12]. Second, vertebrates at the earliest life stages are often more responsive to perturbation [13–16]. Highly coordinated cell-to-cell communications and molecular signalling are required for normal development. Nanomaterials that interact with molecular signalling pathways, intercellular interactions, or normal cellular processes can be identified by evaluating the response of actively developing organisms to nanomaterial exposure [16].

3. Nanomaterials evaluated

Carbon fullerenes (C_{70}, C_{60} and hydroxylated C_{60}) have proposed uses in fuel cells, groundwater remediation, cosmetics and drug delivery. C_{70} is a common by-product of C_{60} synthesis, and will therefore likely be found in products containing C_{60} unless extensive

purification steps are taken. C_{70} is slightly larger than C_{60}, as it contains 10 more carbon atoms than C_{60}. Similarly to C_{60}, hydroxylated C_{60} has proposed uses in groundwater remediation and drug delivery [17,18]. To investigate the relative importance of size and surface functionalisation on the toxic potential of nanomaterials, we evaluated fullerene toxicity in embryonic zebrafish.

Gold nanoparticles (AuNPs) were also used to test the influence of size and surface functionalisation on toxic potential. These materials have potential applications in optics, electronics, *in vivo* molecular imaging and therapeutics. During the last decade, methods have been developed to synthesise a library of ligand-functionalised AuNPs that have precise size, shape and purity [19,20]. Our choice of two core sizes (0.8 and 1.5 nm) with one of three surface groups [neutral charge = 2-(2-mercaptoethoxy)ethanol (MEE), positive charge = *N*, *N*, *N*-trimethylammoniumethanethiol (TMAT), and negative charge = 2-mercaptoethanesulfonate (MES)] allowed us to also investigate the influence nanoparticle charge on toxic potential.

To investigate the importance of chemical composition on nanoparticle–biological interactions, we evaluated 11 commercially available dispersions of noncoated nanoparticulate metal oxides [*positively charged* – aluminum oxide (Al_2O_3; CAS #1344-28-1), titanium (IV) oxide (TiO_2); CAS #13463-67-7), zirconium (IV) oxide (O_2Zr; CAS #1314-23-4), gadolinium (III) oxide (Gd_2O_3; CAS #12064-62-9), dysprosium (III) oxide (Dy_2O_3; CAS #1308-87-8), holmium (III) oxide (H_2 O_3; CAS #12055-62-8), samarium (III) oxide (Sm_2O_3; CAS #12060-58-1), and erbium (III) oxide (Er_2O_3; CAS #12061-16-4)], and [*negatively charged* – yttrium (III) oxide (Y_2O_3; CAS #1314-36-9), silicon dioxide, alumina doped (SiO_2/Al_2O; CAS #7631-86-9), and cerium (IV) oxide (CeO_2; CAS #1306-38-3)]. Primary particle sizes and the size of agglomerates in nanoparticulate metal oxide dispersions at 50 ppm were determined by photon correlation spectroscopy (PCS). Fundamentally, PCS measures the rate of diffusion of particles through fluid and uses that rate and the principles of Brownian motion to determine the distribution of particle sizes. Mean particle size, the range of particle sizes and the predominant particle size are graphically represented in Figure 1. Notably, TiO_2, CeO_2, Dy_2O_3, Sm_2O_3, and Er_2O_3 form large agglomerates. Of the metal oxides that form these large agglomerates, only Er_2O_3 was found primarily in that state.

We chose to evaluate commercially available materials for two important reasons. First, nanoparticles produced on a large scale are not expected to be pure. Second, nanoparticles that are currently commercially available are already being used for industrial applications [21]. Nano-sized metals and metal oxides have unique properties useful for novel applications in electronics, healthcare, optics, technology, and engineering industries. Some metallic nanoparticles, particularly bimetallics, are currently being tested for remediation of organic groundwater contamination, chelation of toxic metals and *in vivo* biomedical imaging. Nanoparticulate metal oxides also offer many advantages for sensors, catalysis and microelectronics applications.

In vivo biodistribution of nanomaterials was investigated using polystyrene and CdSe fluorescent nanomaterials (FluoSphere® and Qdots®, respectively). Qdots® (605ITK-carboxyl QDs, 605ITK-amino (PEG) QDs and 605ITK-organic QDs) were generously donated by, and FluoSpheres® (0.02 μm sulfate, carboxylate, and aldehyde-sulfate modified fluorescent spheres) were purchased from Invitrogen/Molecular Probes (Eugene, OR). Both nanomaterials have novel applications in the fields of biomedical

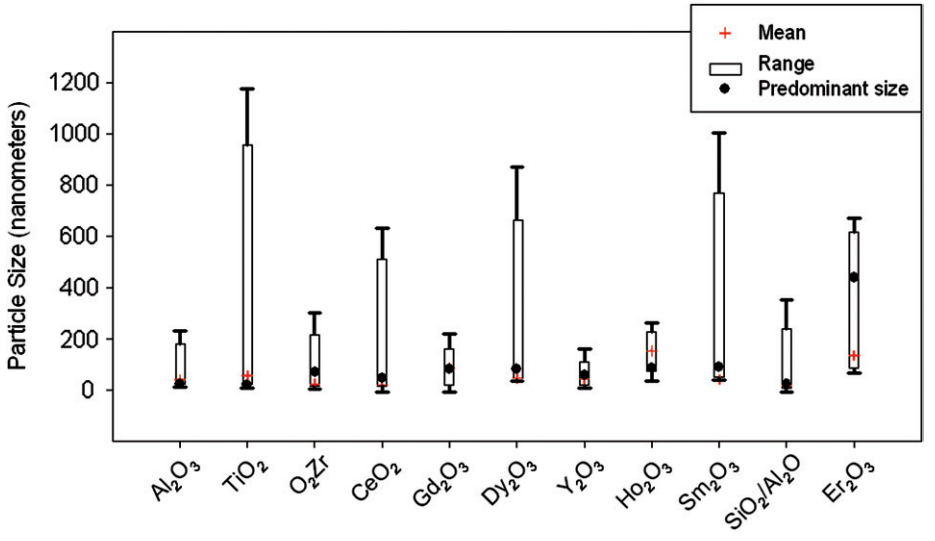

Figure 1. Mean size (crosshairs), the range (box) of particle sizes with error bars representing SD, and the predominant particle size (black circle; percentage at that size) are shown for each metal oxide. Measurements were made using PCS at a concentration of 50 ppm.

imaging, drug delivery and electronics. These engineered materials demonstrate a wide range of physicochemical properties dependent upon inherent characteristics and environmental conditions. The intent of these studies was to identify how those properties and route of exposure affected nanoparticle biodistribution.

4. Experimental design

These studies aimed to investigate the effects of nanomaterial exposure on vertebrate systems using the unique advantages of the embryonic zebrafish model. Screening level toxicological testing was performed to determine *in vivo* responses to, and biological consequences of, nanomaterial exposure. Those results were used to identify inherent physicochemical properties that modulate the biological consequences. Fluorescent nanomaterials were used to investigate how parameters such as surface functionalisation, chemical composition and route of exposure (dermal, injection and oral) influence *in vivo* biodistribution.

4.1. *Exposure protocols for* in vivo *evaluation of toxicity*

AB strain of zebrafish (*Danio rerio*) was reared in the Sinnhuber Aquatic Research Laboratory (SARL) at OSU. Adults were kept at standard laboratory conditions of 28°C on a 14 h light:10 h dark photoperiod. Embryos collected from group spawns were staged for experimental studies. To avoid barrier effects posed by the chorion (egg membrane), embryos staged at 6 hpf (hours post-fertilisation) were dechorionated using pronase enzyme degradation. Nanomaterials were dispersed in water, except for the fullerenes,

which were sonicated in 100% dimethyl sulfoxide and diluted to a 1% final concentration [14,15]. Control animals for the fullerene evaluations were exposed to 1% DMSO. To simulate dermal exposure, 8 hpf embryos were continuously waterborne exposed in individual wells of 96-well plates ($N = 24$ per treatment) until 120 hpf. Exposures were started at 8 hpf to ensure coverage of gastrulation and organogenesis, the periods of development were most well conserved among vertebrates. For injection exposures, 8 hpf embryos were arranged in agarose molds and injected with 2.3 nL nanomaterial solution using a picoliter injection system. Control embryos were sham injected with vehicle lacking nanoparticles. After injection, embryos were transferred to fish water in wells of a 96-well plate and incubated at 28°C until 120 hpf.

4.2. *Biodistribution of nanomaterials*

Since distribution patterns were expected to depend on the route of exposure, we employed three different modes of administering FluoSphere® (40 ppm; 20 nm; Molecular Probes, Eugene, OR) and Qdots® (2 nM; 20 nm; Molecular Probes, Eugene, OR) to embryos. To simulate dermal exposure, embryos were continuously exposed from 8–96 hpf in individual wells of a 96-well plate. Uptake via ingestion (oral route) was evaluated in animals waterborne exposed later in development (144–168 hpf) when the larvae is actively feeding, and dermal tissues are less permeable. The third route of exposure we considered was injection. Microinjections were performed at 8 hpf on embryos with intact chorion. After injection, embryos were allowed to mature to 120 hpf. For evaluations, embryos were anaesthetised with tricaine and mounted on a glass cover slip in 3% methyl cellulose. Embryos were visualised using an inverted fluorescent microscope and images were digitally captured.

5. Evaluation of nanomaterial–biological interactions and responses

The principal characteristics that may be predictive of nanoparticle–biological interactions have yet to be identified. In these studies, we exposed embryonic zebrafish to a variety of nanomaterials and evaluated the incidence of mortality, morphological malformations, behavioural abnormalities and delayed development.

5.1. *Influence of nanomaterial size and surface functionalisation*

Our evaluations of exposure to graded concentrations of fullerenes [C_{60}, C_{70}, and $C_{60}(OH)_{24}$] revealed that surface functionalisation had a greater effect on toxicity than size [22,23]. Exposure to C_{60} and C_{70} significantly increased mortality and the incidence of pericardial edema and fin malformations, while the response to $C_{60}(OH)_{24}$ exposure was less pronounced even at concentrations an order of magnitude higher. These observed differences could also be due to differences in agglomeration status of the fullerene solutions. Hydrophobic nanoparticles, such as C_{60} and C_{70}, tend to agglomerate in water or other hydrophilic media and could be present as huge macroscopic agglomerates, regardless of their primary particle size.

Core size and surface functionalisation, both influenced the toxicity of AuNPs. We found a strong dependence on surface charge and a moderate influence of

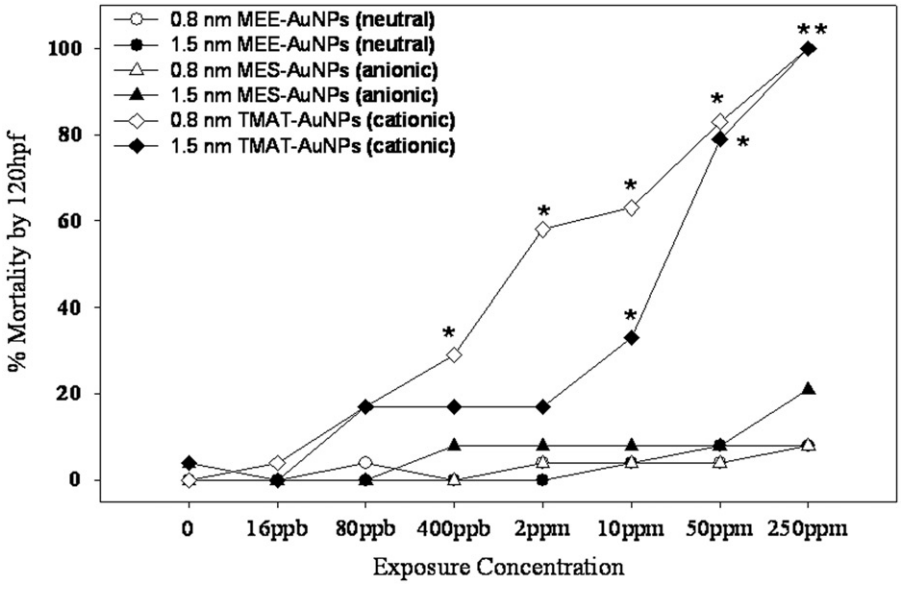

Figure 2. Cumulative percent mortality of embryonic zebrafish ($N = 24$ per group) waterborne exposed to 0.8 Enm(open symbols) and 1.5 nm (closed symbols) AuNPs functionalised with neutral (circles), anionic (triangles) or cationic (diamonds) surface groups. Mortality reported as percent of embryos that had died by 120 hpf. Significant difference from control (concentration 0) was determined using Fisher's Exact test ($*p < 0.05$).

particle diameter. Exposure to positively charged TMAT, AuNPs resulted in significantly higher toxicity than did negatively charged particles, while neutral particles exhibited no toxicity. AuNPs functionalised with TMAT caused a significant increase in mortality at 10 ppm (parts per million) for 1.5 nm particles and 400 ppb (parts per billion) for 0.8 nm particles (Figure 2). Exposure to MES–AuNPs did not result in increased mortality at concentrations up to 250 ppm; however, concentrations of 2 and 50 ppm did result in increased incidence of morphological malformations at 1.5 and 0.8 nm particles, respectively (data not shown). Embryos exposed to 1.5 nm TMAT functionalised nanoparticles also displayed increased incidences of malformations at 50 ppm. Such malformations were observed at a much lower concentration (80 ppb) when the TMAT–AuNP size was 0.8 nm.

5.2. *Influence of chemical make-up and route of exposure*

Of 11 metal oxide nanoparticulates tested, approximately half were benign to embryonic zebrafish after a 5-day continuous waterborne exposure at concentrations ranging from 16 ppb to 250 ppm. Significant mortality was observed at 50 ppm for Er_2O_3 and Sm_2O_3, and at 250 ppm for Ho_2O_3 and Dy_2O_3 (Figure 3, Al_2O_3 and TiO_2 shown to illustrate a nonresponse). Significant morphological malformations were also induced by waterborne exposure to Er_2O_3, Sm_2O_3 and Dy_2O_3 at concentrations of 10, 50 and 250 ppm, respectively (Figure 4). Exposure to Sm_2O_3 significantly increased the incidence of jaw, heart, eye and snout malformations at 50 ppm. Exposure to SiO_2/Al_2O resulted in

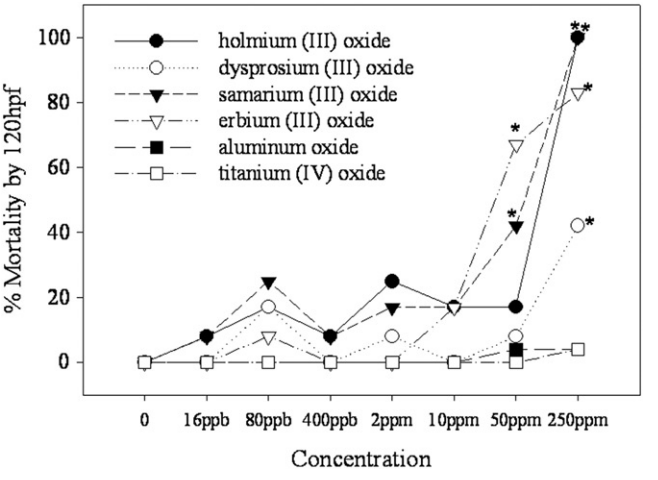

Figure 3. Cumulative percent mortality of zebrafish embryos ($N = 24$ per group) waterborne exposed to holmium (III) oxide (●), dysprosium (III) oxide (○), samarium (III) oxide (▼), erbium (III) oxide (▽), aluminum oxide (■) and titanium (IV) oxide (□). Mortality reported as percent of embryos that had died by 120 hpf. Significant difference from control (concentration 0) was determined using Fisher's Exact test (*$p < 0.05$).

a significant incidence of jaw malformations at 250 ppm. At 10 ppm, Er_2O_3 exposure elicited jaw malformations in 44% of embryos after 5 days. Exposure to 50 ppm Er_2O_3 significantly increased the incidence of jaw, heart, eye, snout, trunk and body axis malformations. Dy_2O_3 exposure significantly affected the jaw and eyes at 250 ppm. Embryonic exposure to Y_2O_3 significantly increased the incidence of jaw malformations at 10 ppm and the incidence of jaw and heart malformations of embryos exposed to 250 ppm.

Microinjections of metal oxide nanoparticle dispersions were administered to embryonic zebrafish to test the effects of exposure via an injection route. Morphological malformations elicited by waterborne exposure to nanoparticulate metal oxides were mimicked by injection exposures for Sm_2O_3 (Figure 5) and Y_2O_3 (Figure 6). No significant morbidity or mortality was observed from any of the nanoparticulate metal oxides when embryos were injected with approximately 0.5 ng nanoparticles (0.5 ug g^{-1} dose).

5.3. *Biodistribution evaluations*

In vivo distributions were determined for embryonic zebrafish exposed (waterborne, injection, oral) to fluorescent FluoSphere® and Qdots® in order to evaluate the influence of exposure route and surface functionalisation on uptake and biodistribution. A timeline for uptake from waterborne exposures was determined for FluoSphere® with carboxylated surface functionalisation. Waterborne FluoSpheres® were observed in external epithelial tissues for the first 24 h, in the vasculature by 72 h and in the digestive tract by 144 h. Distribution after uptake appeared to be greater for Qdots® than for FluoSpheres®, independent of the route of exposure (Figure 7). Uptake from a dermal route was primarily limited to the epithelial layers and the yolk sac for carboxylated FluoSpheres®, but distribution to the brain region was achieved from waterborne exposure to Qdots®.

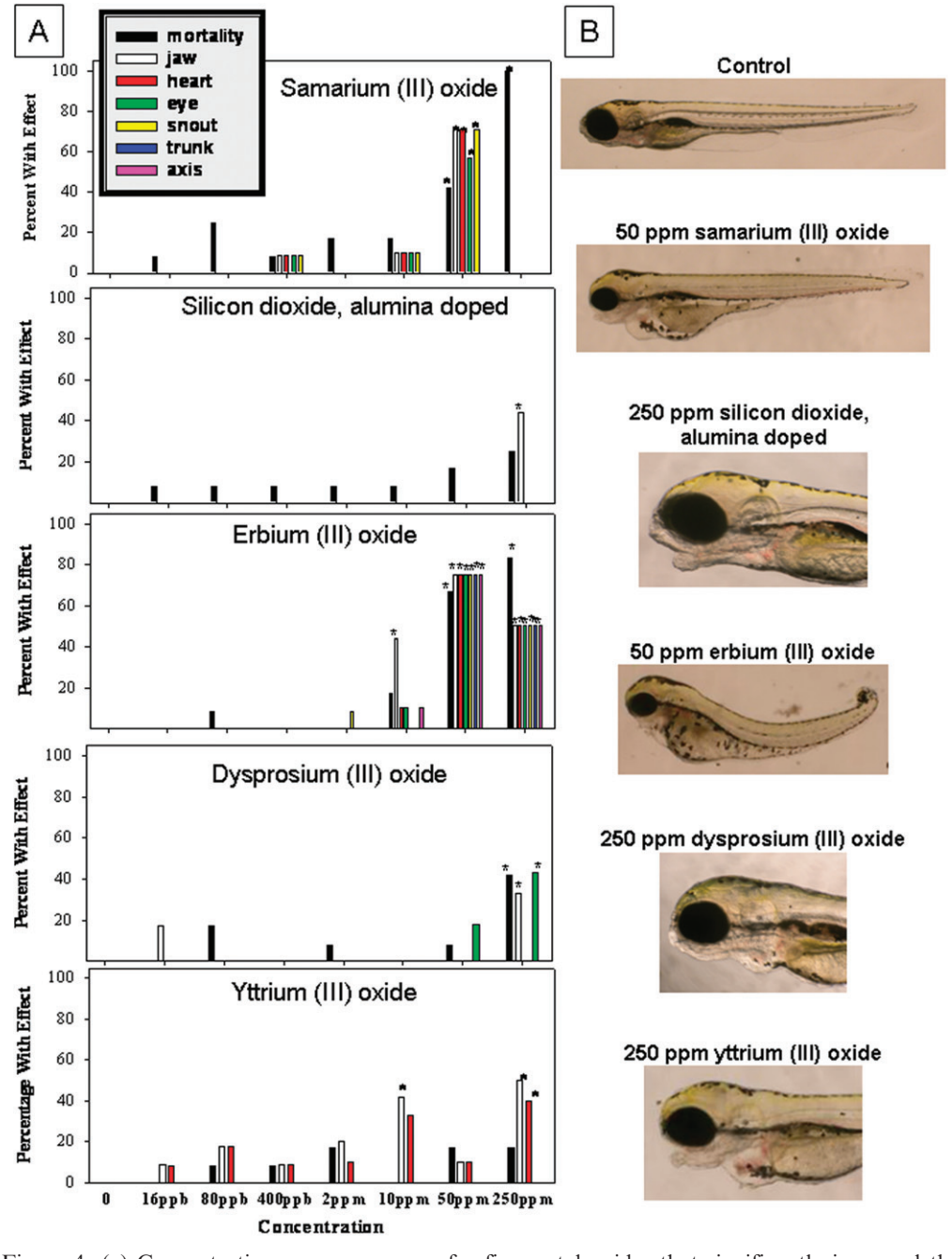

Figure 4. (a) Concentration–response curves for five metal oxides that significantly increased the incidence of malformations ($N = 24$ per treatment). Values represent the cumulative percent of animals with effect by 120 hpf. Mortality reported as percent of embryos that had died by 120 hpf. Significant difference from control (concentration 0) was determined using Fisher's Exact test ($^*p < 0.05$). (b) Bright field images of embryos representative of exposure to nanoparticulate metal oxides.

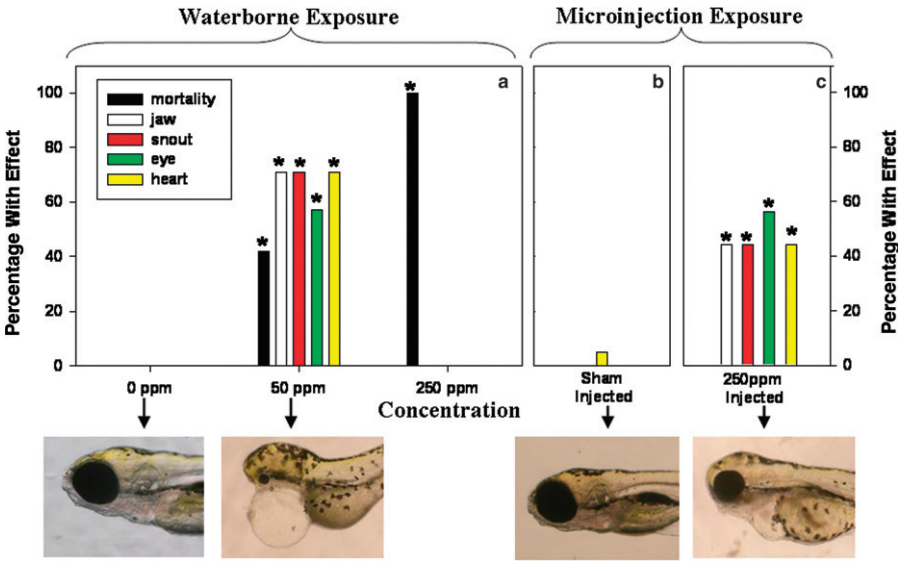

Figure 5. Morbidity and mortality of embryonic zebrafish (a) waterborne exposed to 50 or 250 ppm samarium (III) oxide, (b) sham injected with 2.3 nL water, and (c) microinjected with 2.3 nL of 250 ppm (~0.5 ng) samarium (III) oxide. *Indicates significant difference from waterborne or microinjection control groups using Fisher's Exact test ($p < 0.05$).

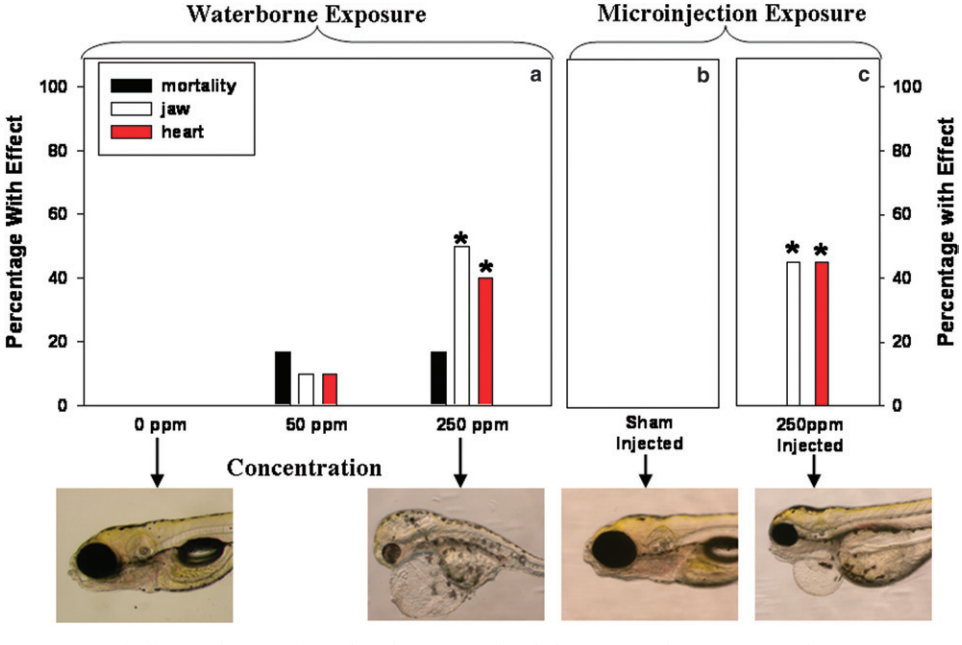

Figure 6. Morbidity and mortality of embryonic zebrafish (a) waterborne exposed to 50 or 250 ppm yttrium (III) oxide, (b) sham injected with 2.3 nL water, and (c) microinjected with 2.3 nL of 250 ppm (~0.5 ng) yttrium (III) oxide. *Indicates significant difference from waterborne or microinjection control groups using Fisher's Exact test ($p < 0.05$).

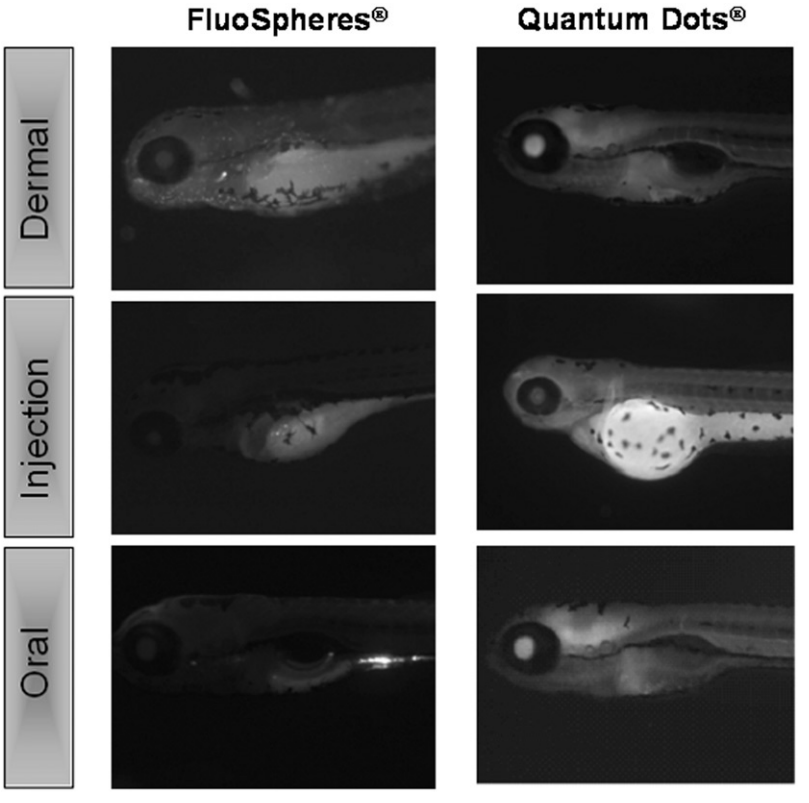

Figure 7. Biodistribution of FluoSpheres® and QDots® administered via waterborne (dermal and oral) or microinjection (injection) exposure. Exposures were conducted from 8 to 120 hpf to represent a dermal route and from 120 to 144 hpf to represent an oral route. Microinjections were done at 8 hpf.

Microinjection route also shows differential uptake and distribution. FluoSpheres® administered via the oral route of exposure were retained within the gastrointestinal tract; whereas, Qdots® were readily taken up across the gastrointestinal tract and distributed to the brain. A comparison of 20 nm carboxylate-modified Qdots® and FluoSpheres® revealed a strong influence of chemical composition on distribution independent of the surface functional groups.

6. Conclusions

Immense data gaps and conflicting reports on nanotoxicology currently prevent generalising how nanoparticle physicochemical properties relate to biological activity and toxic potential. *In vivo* animal models, such as the zebrafish, are needed to interpret the effects of nanomaterial exposure in a whole animal context. The size differences we evaluated using carbon fullerenes and AuNPs were relatively small and thus limits our interpretation of the influence of size on nanomaterial toxic potential. Surface functionalisation significantly affected toxicity of fullerenes and AuNPs yet did not

dictate the biodistribution of fluorescent nanoparticles. Biodistribution was instead influenced by chemical composition and the route of exposure. Chemical composition significantly influenced the toxicity of nanoparticulate metal oxides but the influence of exposure route was less pronounced, perhaps due to the amount injected. Overall, our results indicate that the zebrafish model is a powerful platform to help unravel nanomaterial structure and biological response relationships.

Acknowledgements

The authors would like to thank Dr Chih-Hung Chang and Yu-Jen Chang of the Department of Chemical Engineering at OSU for their assistance with PCS. These studies were partially supported by the Oregon State University Research Office, the Safer Nanomaterials and Nanomanufacturing Initiative of the Oregon Nanoscience and Microtechnologies Institute grant FA8650-05-1-5041, EPA STAR grant RD-833320, and NIEHS grants ES03850 and ES07060.

References

[1] G.E. Ackermann and B.H. Paw, *Zebrafish: a genetic model for vertebrate organogenesis and human disorders*, Front. Biosci. 8 (2003), pp. d1227–d1253.
[2] A.J. Hill, H. Teraoka, W. Heideman, and R.E. Peterson, *Zebrafish as a model vertebrate for investigating chemical toxicity*, Toxicol. Sci. 86 (2005), pp. 6–19.
[3] L.K. Mathew, E.A. Andreasen, and R.L. Tanguay, *Aryl hydrocarbon receptor activation inhibits regenerative growth*, Mol. Pharmacol. 69 (2006), pp. 257–265.
[4] J. Spitsbergen and M. Kent, *The state of the art of the zebrafish model for toxicology and toxicologic pathology research – advantages and current limitations*, Toxicol. Pathol. 31 (2003), pp. 62–87.
[5] R.L. Brent, *Utilization of juvenile animal studies to determine the human effects and risks of environmental toxicants during postnatal development*, Birth Defects Res. (Part B) 71 (2004), pp. 303–320.
[6] A.L. Rubinstein, *Zebrafish: from disease modeling to drug discovery*, Curr. Opin. Drug Discov. Develop. 6 (2003), pp. 218–223.
[7] C.B. Kimmel, W.W. Ballard, S.R. Kimmel, B. Ullmann, and T.F. Schilling, *Stages of embryonic development of the zebrafish*, Develop. Dyn. 203 (1995), pp. 253–310.
[8] J.M. Bates, E. Mittge, J. Kuhlman, K.N. Baden, S.E. Cheesman, and K. Guillemin, *Distinct signal from the microbiota promote different aspects of zebrafish gut differentiation*, Dev. Biol. 297 (2006), pp. 374–386.
[9] S. Aparicio, J. Chapman, E. Stupka, N. Putnam, J.M. Chia, P. Dehal, A. Christoffels, S. Rash, S. Hoon, A. Smit et al., *Whole-genome shotgun assembly and analysis of the genome of Fugu rubripes*, Science 297 (2002), pp. 1301–1310.
[10] F. Busquet, R. Nagel, F. von Landenberg, S.O. Mueller, N. Huebler, and T.H. Broschard, *Development of a new screening assay to identify proteratogenic substances using zebrafish danio rerio embryo combined with an exogenous mammalian metabolic activation system (mDarT)*, Toxicol. Sci. 104 (2008), pp. 177–188.
[11] D.B. Henken, R.S. Rasooly, L. Javois, and T.I. Hewitt, *Recent papers on zebrafish and other aquarium fish models*, Zebrafish 1 (2003), pp. 305–311.
[12] P. Lein, E. Silbergeld, P. Locke, and A.M. Goldberg, In vitro *and other alternative approaches to developmental neurotoxicity testing (DNT)*, Environ. Toxicol. Pharmacol. 19 (2005), pp. 735–744.

[13] National Research Council (NRC), Scientific frontiers in developmental toxicology and risk assessment. In: *Board on Environmental Studies and Toxicology*, National Academy Press: Washington, DC, 2000, pp. 1–327.
[14] S.R. Blechinger, J.T. Warren Jr, J.Y. Kuwada, and P.H. Krone, *Developmental toxicology of cadmium in living embryos of a stable transgenic zebrafish line*, Environ. Health Perspect. 110 (2002), pp. 1041–1046.
[15] S. Bretaud, S. Lee, and S. Guo, *Sensitivity of zebrafish to environmental toxins implicated in Parkinson's disease*, Neurotoxicol. Teratol. 26 (2004), pp. 857–864.
[16] S.L. Harper, J.L. Dahl, B.L.S. Maddux, R.L. Tanguay, and J.E. Hutchison, *Proactively designing nanomaterials to enhance performance and minimize hazard*, Int. J. Nanotechnol. 5 (2008), pp. 124–142.
[17] E. Nakamura and H. Isobe, *Functionalized fullerenes in water. The first 10 years of their chemistry, biology, and nanoscience*, Acc. Chem. Res. 36 (2003), pp. 807–815.
[18] R. Anderson and A.R. Barron, *Reaction of hydroxyfullerene with metal salts: a route to remediation and immobilization*, J. Am. Chem. Soc. 127 (2005), pp. 10458–10459.
[19] G.H. Woehrle, L.O. Brown, and J.E. Hutchison, *Thiol-functionalized, 1.5-nm gold nanoparticles through ligand exchange reactions: scope and mechanism of ligand exchange*, J. Am. Chem. Soc. 127 (2005), pp. 2172–2183.
[20] G.H. Woehrle and J.E. Hutchison, *Thiol-Functionalized Undecagold Clusters by Ligand Exchange: Synthesis, Mechanism, and Properties*, Inorg. Chem. 44 (2005), pp. 6149–6158.
[21] P. Cherukuri, S. Bahilo, S. Litovsky, and R. Weisman, *Near-infrared fluorescence microscopy of single-walled carbon nanotubes in phagocytic cells*, J. Am. Chem. Soc. 126 (2004), pp. 15638–15639.
[22] C.Y. Usenko, S.L. Harper, and R.L. Tanguay, *In vivo evaluation of carbon fullerene toxicity using embryonic zebrafish*, Carbon 45 (2007), pp. 1891–1898.
[23] C.Y. Usenko, S.L. Harper, and R.L. Tanguay, *Exposure to fullerene C60 elicits an oxidative stress response in embryonic zebraflsh*, Toxicol. Appl. Pharmacol. (2008), pp. 44–55.